An Integration-Friendly Regrowth-Free Tunable Laser

Ludovic Caro, Mohamad Dernaika, Niall P. Kelly, Padraic E. Morrissey, Justin K. Alexander, and Frank H. Peters

***Abstract*— This letter presents a single-mode tunable laser operating in the *L*-band. The facetless design, along with a regrowth-free fabrication that does not require high-resolution lithography techniques, contributes to make the laser a suitable candidate for monolithic integration with other components. Tuning is demonstrated over a range of 47 nm, with side-mode suppression ratio values over 30 dB and a linewidth of 800 kHz.**

***Index Terms*— Photonic integrated circuits.**

I. Introduction

MODERN communication networks rely heavily on single-mode tunable lasers for multi-wavelength communication systems. Single-mode is often achieved by using grating-based lasers such distributed Bragg reflectors (DBR) lasers [1], sampled grating DBR (SGDBR) lasers [2], or distributed feedback (DFB) lasers [3]. However, such lasers often require multiple epitaxial growth steps and high-resolution lithography [4]. While regrowth-free DFB lasers have been reported [5], [6], they require holographic lithography that increases the cost compared to standard UV lithography. A regrowth-free alternative has been proposed as a means to achieve single mode, that is also based on standard UV lithography: the introduction of defects along the laser cavity to create intra-cavity resonance leading to single-mode operation. Such defects can be slots [7], in slotted Fabry-Perot (SFP) lasers. However, their reflection and transmission performance proved to be sensitive to etch depth, thus requiring careful control and potentially reducing the fabrication yield [8].

Another limitation observed in single-mode tunable lasers is the presence of cleaved facets as reflective features providing feedback. Such cleaved facets, also present in some DBR or SGDBR lasers [9], [10], add significant constraints to the development of monolithic photonic integrated circuits (PICs), limiting the options as to where the light source can be positioned: if the laser relies on a cleaved facet, it has to be placed at the edge of the chip.

The device presented here is a regrowth-free facetless laser using multimode interference (MMI) couplers [11] to couple parallel cavities terminated by on-chip, gold-coated etched facets (metal on etched facet, MEF) [12]. The use of an MMI coupler makes it possible to allocate one of the MMI ports to the guiding of the laser output towards other components, making the monolithic integration of this device with other components, trivial.

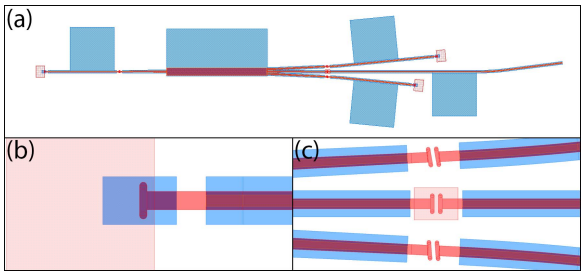

Fig. 1. (a) Schematic of the proposed design with details of (b) a MEF and (c) shallow isolation and deep reflective slots.

II. Proposed Design

The proposed design consists of a central 3×3 MMI coupler, to which several arms are connected. On one side, a single waveguide connected to the central port is terminated by a MEF and acts as a common section for the multiple cavities of the design. On the other side, a central arm acts as an output coupler and includes a reflective slot to provide a feedback boost, while two arms, also terminated by MEFs but of different lengths, are connected to the two outer ports. By interfering with each other, the two cavity lengths (here 870μm and either 920μm or 970μm) generate super-modes of predictable spacing [13], and enable single-mode operation. The resulting design is presented in Figure 1. The output port was angled compared to the cleave plan to avoid any parasitic reflections during the characterisation process.

The 3×3 MMI coupler is 226μm long and 17μm wide. If an input signal is applied to the central port on one side of this coupler, this signal will be equally split between the three ports on the other side of the coupler, as described in [14]. As a result, it is also possible, under the right phase and amplitude conditions, to use this property to recombine three beams into a single port. In the proposed design, achieving the optimal recombination conditions requires feedback from the output arm of the laser. This is why a reflective slot was used on this arm, providing a reflectivity of approximately 20% [15]. However, because it is not a critical feature for single mode lasing, the slot depth does not require the careful control necessary for SFP lasers.

Manuscript received June 23, 2017; revised September 8, 2017; accepted December 6, 2017. Date of publication December 11, 2017; date of current version January 15, 2018. This work was supported by the Science Foundation Ireland under Grant SFI 10/CE/I1853 (CTVR2) and Grant SFI 13/IA/1960. *(Corresponding author: Ludovic Caro.)*

L. Caro, M. Dernaika, N. P. Kelly, J. K. Alexander, and F. H. Peters are with the Integrated Photonics Group, Tyndall National Institute, T12 R5CP Cork, Ireland, and also with the Physics Department, University College Cork, T12 YN60 Cork, Ireland (e-mail: ludovic.caro@tyndall.ie).

P. E. Morrissey is with the Integrated Photonics Group, Tyndall National Institute, T12 R5CP Cork, Ireland.

Color versions of one or more of the figures in this letter are available online at http://ieeexplore.ieee.org.

Digital Object Identifier 10.1109/LPT.2017.2781799

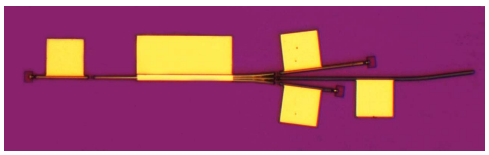

Fig. 2. Microscope photograph of a fabricated device.

Through the use of on-chip etched facets and the availability of a waveguide to collect and direct the laser output to any other devices, the proposed design facilitates the monolithic integration of other components with the laser to obtain complex PICs at reduced cost and process complexity [16].

A design based on similar technologies was presented in [13], but it suffers a flaw due to the 2×2 MMI coupler that sends 50% of the power towards the output coupler at each round-trip. This causes a decrease in efficiency, output power and side-mode suppression ratio (SMSR). The use of a 3×3 coupler limits this loss to a theoretical maximum of 33%, which is then reduced further using a deeply etched mirror in the output arm.

III. Fabrication Process

The material used to fabricate the device was commercially obtained 1550nm laser material, grown on an InP substrate. It includes 5 compressively strained AlInGaAs quantum wells and does not involve any regrowth step in its construction. The fabrication process, similar to the one presented in [17], is exclusively based on standard UV lithography. Using a combination of silicon oxide and silicone nitride layers as hard masks, it is possible to achieve two different etch depths, one immediately above the quantum wells to define the waveguides, and one below the quantum wells to improve the MEF and slot reflectivity. The metal contacts consist of Ti:Au (20:250nm) deposited by electron beam evaporation. They were patterned by the means of standard lift-off lithography, and the evaporation used a 360° tool to ensure adequate deposition on the side walls, especially on the MEFs. The resulting devices are presented in Figure 2.

With a simple fabrication process involving two etch depths and no advanced lithography techniques, the proposed devices are highly compatible with standard shared foundry processes [16]. With the integration-friendly geometry, they are good candidates as light sources for large-scale production of PICs.

IV. Characterization Results

The device was characterised on a temperature controlled brass chuck that was maintained constant at 20°C by the means of a thermoelectric cooler. The light output was collected from an angled output waveguide through a lensed fibre, to further reduce parasitic reflections that could disturb the analysis of the results. The total threshold current was of approximately 150mA, and the laser total output power was in the -10dBm (0.1mW) range.

A. Tuning Performance

The devices presented here achieved a tuning range of 47nm. The interference between the multiple cavities in the device causes an envelope to shape the emission spectrum into a series of super-modes. This interference, and therefore the location of the super-modes can be altered by the thermally induced refractive index change caused by altering the current in the different sections of the laser. Similarly, the gain peak of the laser is thermally adjusted by altering the current in the laser. While, these effects are not independent, it is still possible to modify the position of the maximum gain of the laser, from one super-mode to the next, to tune the lasing wavelength. Indeed, the gain shift is significantly faster than the envelope shift, as can be observed in Figure 3 between the 1585nm and 1591nm lasing wavelengths. To cover the wavelength range reported from 1564nm to 1611nm, injection currents from 80mA to 250mA were applied to the MMI section, and from 20mA to 65mA to the different waveguide sections. Then, because the MMI section was common to all resonant cavities, a smaller adjustment of the current through this section led to the fine tuning of the laser. The choice of the MMI coupler over the common waveguide section is due to the coupler, being significantly larger and thus less thermally sensitive to the injection current, enables a finer tuning.

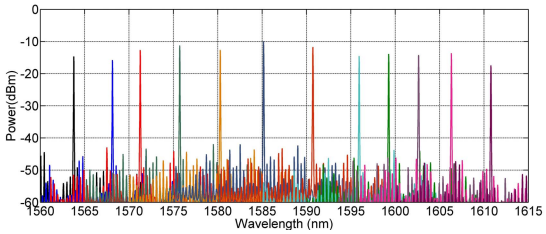

Fig. 3. Emission spectra of a 1x3 MMI/MEF laser for a 100μm cavity length difference.

The lasing spectra of a device at various bias configurations are shown in Figure 3, illustrating the achieved tuning range. The side-mode suppression ratio (SMSR) values for the spectra shown in Figure 3 were maintained above 30dB, reaching up to 33dB for the 1585nm lasing wavelength.

Fine tuning was also achieved by adjusting the injection current through the MMI coupler. Given the super-mode spacing inherent to the cavity length difference, the fine tuning range is related to the super-mode spacing: the shorter the length difference, the wider the spacing and the lower the tendency of the laser to switch to a different super-mode. As a result, wider local tuning ranges are achieved for smaller arm length differences. In the case of a 50μm difference, a fine tuning range of up to 3nm was observed, with SMSR values above 27dB, as shown in Figure 4.

B. Laser Characterisation

The lasing spectra were processed by a Fourier analysis tool to study the spectrum and extract data on the cavities involved on the observed laser signal. Such an analysis is presented in Figure 5. The peaks on the graph correspond to the lengths of the cavities leading to the emitted spectrum. The two main peaks, at approximately 870μm and 970μm, correspond to the two cavities defined by the top and bottom arms of the laser. This 100μm length difference can also be observed at

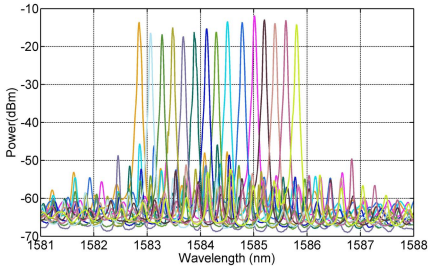

Fig. 4. Fine tuning of a 1x3 MMI/MEF laser for a 50μm cavity length difference.

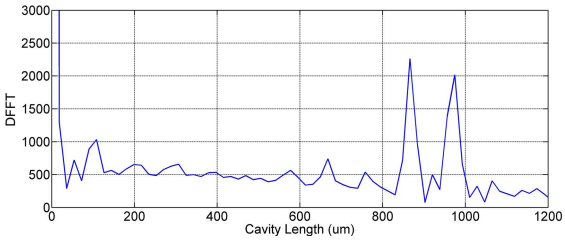

Fig. 5. Fourier analysis of the laser spectrum for a 100μm length difference.

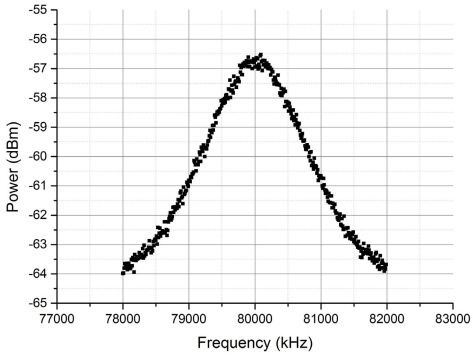

Fig. 6. Self-interference profile of the laser emission spectrum.

the 100μm peak. One can also observe minor peaks at 560μm, 660μm and 760μm.

The signal conditions for the MMI in [14] described relative values of phase and amplitude for correct recombination of the inputs into a single output beam. When these conditions are not met, light is present at the unallocated MMI ports, on each side of the common arm. In the absence of an output waveguide, this light is reflected back into the MMI, leading to the 560μm and 660μm reflections. Their combination with the 100μm length difference causes the artifact at 760μm. Indeed, these lengths correspond to the separation from the two MEFs to the opposite end of the MMI coupler.

The linewidth of the laser was measured using a standard self-heterodyne technique using a 50km fiber as delay [18]. The interference profile (Figure 6) shows a full-width at half-maximum of 1.6MHz, corresponding to a linewidth of 800kHz. This value of linewidth is similar to that of the laser proposed in [13], however the SMSR, the tuning range, and the output power of the laser presented here have been significantly improved from the previous work.

V. Conclusion

An MMI-based laser design was proposed and demonstrated. It can be fabricated from regrowth-free material, through a two-depth process that does not require advanced lithography techniques. The fabrication simplicity, along with the facetless design, make it a suitable canditate for monolithic integration into PICs. A tuning range of 47nm was achieved with SMSR values above 30dB, as well as fine local tuning. The laser linewidth was measured to be 800kHz.

References

[1] K. Utaka, K. Kobayashi, and Y. Suematsu, "Lasing characteristics of 1.5–1.6 μm GaInAsP/InP integrated twin-guide lasers with first-order distributed Bragg reflectors," *IEEE J. Quantum Electron.*, vol. QE-17, no. 5, pp. 651–658, May 1981.

[2] S.-L. Lee, I.-F. Jang, C.-Y. Wang, C.-T. Pien, and T.-T. Shih, "Monolithically integrated multiwavelength sampled grating DBR lasers for dense WDM applications," *IEEE J. Sel. Topics Quantum Electron.*, vol. 6, no. 1, pp. 197–206, Jan. 2000.

[3] M. Nakamura, H. W. Yen, A. Yariv, E. Garmire, S. Somekh, and H. L. Garvin, "Laser oscillation in epitaxial GaAs waveguides with corrugation feedback," *Appl. Phys. Lett.*, vol. 23, no. 5, pp. 224–225, 1973.

[4] J. Buus, M.-C. Amann, and D.-J. Blumenthal, *Tunable Laser Diodes and Related Optical Sources*. Hoboken, NJ, USA: Wiley, 2005.

[5] J. Wang, J.-B. Tian, P.-F. Cai, B. Xiong, C.-Z. Sun, and Y. Luo, "1.55-μm AlGaInAs-InP laterally coupled distributed feedback laser," *IEEE Photon. Technol. Lett.*, vol. 17, no. 7, pp. 1372–1374, Jul. 2005.

[6] S. J. Jang, C. I. Yeo, J. S. Yu, and Y. T. Lee, "1.55-μm DFB lasers with narrow ridge stripe and second-order metal surface gratings by holographic lithography," *Phys. Status Solidi A*, vol. 207, no. 8, pp. 1982–1987, 2010.

[7] B. Corbett, C. Percival, and P. Lambkin, "Multiwavelength array of single-frequency stabilized Fabry-Perot lasers," *IEEE J. Quantum Electron.*, vol. 41, no. 4, pp. 490–494, Apr. 2005.

[8] Q. Y. Lu *et al.*, "Analysis of slot characteristics in slotted single-mode semiconductor lasers using the 2-D scattering matrix method," *IEEE Photon. Technol. Lett.*, vol. 18, no. 24, pp. 2605–2607, Dec. 15, 2006.

[9] J. E. Johnson *et al.*, "Fully stabilized electroabsorption-modulated tunable DBR laser transmitter for long-haul optical communications," *IEEE J. Sel. Topics Quantum Electron.*, vol. 7, no. 2, pp. 168–177, Mar. 2001.

[10] C.-L. Yao, S.-L. Lee, I.-F. Jang, and W.-J. Ho, "Wavelength-selectable lasers with Bragg-wavelength-detuned sampled grating reflectors," *J. Lightw. Technol.*, vol. 24, no. 9, pp. 3480–3489, Sep. 2006.

[11] L. B. Soldano and E. C. M. Pennings, "Optical multi-mode interference devices based on self-imaging: Principles and applications," *J. Lightw. Technol.*, vol. 13, no. 4, pp. 615–627, Apr. 1995.

[12] C. Seibert, "High-index-contrast ridge waveguide laser with thermally oxidised etched facet and metal reflector," *Electron. Lett.*, vol. 46, pp. 1077–1078, Jul. 2010.

[13] L. Caro *et al.*, "A facetless regrowth-free single mode laser based on MMI couplers," *Opt. Laser Technol.*, vol. 94, pp. 159–164, Sep. 2017.

[14] K. Cooney and F. H. Peters, "Analysis of multimode interferometers," *Opt. Exp.*, vol. 24, no. 20, pp. 22481–22515, Oct. 2016.

[15] M. Dernaika, L. Caro, N. P. Kelly, and F. H. Peters, "Single facet semiconductor laser with deep etched V-notch reflectors integrated with an active multimode interference reflector," *J. Mod. Opt.*, vol. 64, no. 19, pp. 1941–1946, 2017.

[16] M. Smit *et al.*, "Generic foundry model for inp-based photonics," *IET Optoelectron.*, vol. 5, no. 7, pp. 187–194, 2011.

[17] P. E. Morrissey, N. Kelly, M. Dernaika, L. Caro, H. Yang, and F. H. Peters, "Coupled cavity single-mode laser based on regrowth-free integrated MMI reflectors," *IEEE Photon. Technol. Lett.*, vol. 28, no. 12, pp. 1313–1316, Jun. 15, 2016.

[18] H. Tsuchida, "Simple technique for improving the resolution of the delayed self-heterodyne method" *Opt. Lett.*, vol. 15, no. 11, pp. 640–642, 1990.